Nigerian Journal of Pharmaceutical and Biomedical Research

Vol. 8 Issue.3 December, 2024. p-ISSN: 2579-1419 e-ISSN: 2814-1423

MOLECULAR DOCKING STUDY OF SOME SARS CORONA VIRUS PAPAIN LIKE PROTEASE INHIBITORS

David E. Arthur[1*], Greatman Okafor[2], Adebiyi Adedayo Babafemi[3], Hassan Haruna Umar[1]

[1]Department of Pure and Applied Chemistry, University of Maiduguri P.M.B 1069, Borno-Nigeria
[2]Department of Chemistry, Baze University Abuja, Kano-Nigeria
[3]Sheda Science and Technology complex Abuja, Nigeria

*Correspondence: Tel: +2347015381013, E-mail: eadavid@unimaid.edu.ng
*ORCID: 0000-0002-9823-8847 http://doi.org/10.55639/607.phar.10101.001

Abstract

SARS-CoV-2 PLPro is considered as an important potential target for anti-SAR-CoV-2 drug discovery due to its crucial roles in viral spread. In this study, molecular docking was conducted to compute the scoring function and research protein-ligand interaction of (5-amino-2-methyl-N-(1-(naphthalen-1-yl)ethyl) benzamide, (M1), 2-methyl-4(methylamino)methyl)-N-(1-(naphthalen-1-yl)ethyl)benzamide, (M2), N-(benzo[d][1,3]dioxol-5-ylmethyl)-1-(1-(naphthalen-1-yl)ethyl)piperidine-4-carboxamide, M3), and their derivatives with SARS-Cov2 main protease using Pyrex. The docking result shows that (2-hydroxy-N-(hydroxyl (naphthalen-1-yl)methyl)-4-((hydroxyamino)methyl)benzamide), (M1c), derivative of (5-amino-2-methyl-N-(1-(naphthalen-1-yl)ethyl)benzamide), (M1), has the lowest binding energy with binding score of (-20.411kcal/mol). This show that the compound is very stable and maintains its firm position within the binding pocket of 5Y3Q receptor, indicating that the complex is stable under the varying conditions, thus can be used as inhibitor of SARS Cov2 PLpro.

Key*: Sars-Cov-2, Papain like inhibitors, 5Y3Q receptors,Pyrex tool, Molecular docking*

Introduction

Proteins exert their functions through the recognition of other molecular partners called ligand (Salmaso, 2018). Ligand-protein interactions are involved in many biological processes with Consequent pharmaceutical implications. Thus, the scientific community has been putting a great effort into the investigation of the binding phenomenon during the years, leading to the proposal of several theories characterized by an increasing emphasis on the degree of flexibility of the ligand and protein counterparts. The evolution of binding models has practical relevance besides an epistemological significance; the knowledge of ligand target binding is at the basis of rational drug design but understanding this complex process on a mechanistic level may open new scenarios. In addition, to suggest ligand modification meant to optimize the final bound state, the medicinal chemist may look at kinetically relevant intermediate states and try to affect them (Salmaso and Moro, 2018).

The SARS-CoV-2 pandemic showed the danger of zoonotic viruses for humankind and illustrates the need for the treatment of such diseases. Moreover, the rate of virus mutation indicates the necessity for quick drug search and discovery, which can be facilitated by fast and cost-efficient computational methods. Virtual screening can lead to discovery of potential virus inhibitors or their precursors, either from sets of commonly used therapeutic agents or from naturally occurring compounds.

The process of drug discovery and development for SARS-Cov-2 has been very challenging, time consuming and expensive. Increasing knowledge of drug discovery and as well as increasing computer power has made it possible for the use of computation methods in drug design and discovery. Molecular docking approaches can be used to obtain structural information about promising antiviral compounds for drug discovery and promote savings in the cost of drug design and development, reduce the requirement for lengthy and expensive animal tests and, promote green chemistry to increase efficiency and eliminate chemical waste.

.

Materials and Method

Experiment Data Sets and Ligand Preparation

A workstation system with the following specifications was used: Dual 2.30 GHz CPU, Intel® Core i5-3210M, 6.00GB RAM for this study (Habtemariam, S. 2019), fifteen natural products structures and IUPAC names in Table 1, were identified and chosen from reliable literature. The 2D structures of natural products that showed activity against amyloid beta (A) in the applicability domain of the experimental models used were drawn by Chem-draw software ultra-version 12.0 and thereafter transformed into 3D structures with the aid of Spartan 14 software (Arthur *et al*., 2021). The obtained 3D structures were subsequently optimized geometrically using the DFT approach with the Spartan 14 software package from Wave function Inc. Thereafter, the optimized ligands were saved in pdb file format as prepared ligands for molecular docking simulations study (Arthur *et al*., 2022).

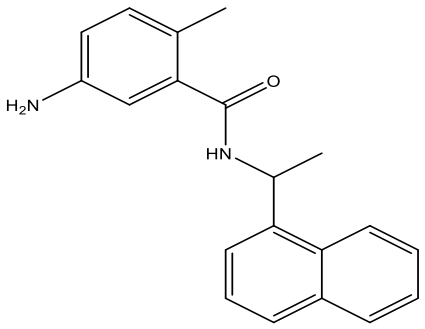

5-amino-2-methyl-*N*-(1-(naphthalen-1-yl)ethyl)benzamide

Figure 1: 2-D structure of the first ligand (M1) with its IUPAC name used in the study.

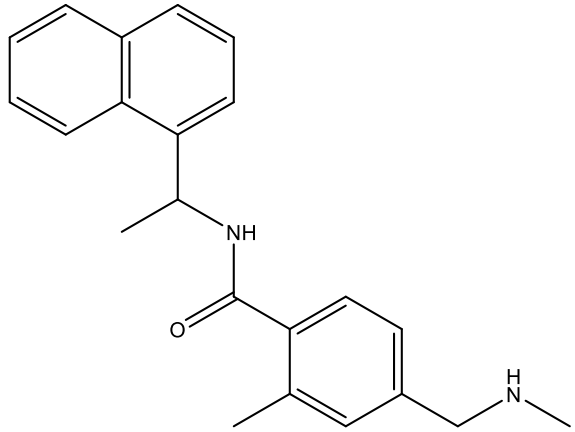

2-methyl-4-((methylamino)methyl)-*N*-(1-(naphthalen-1-yl)ethyl)benzamide

Figure 2: 2-D structure of the first ligand (M2) with its IUPAC name used in the study.

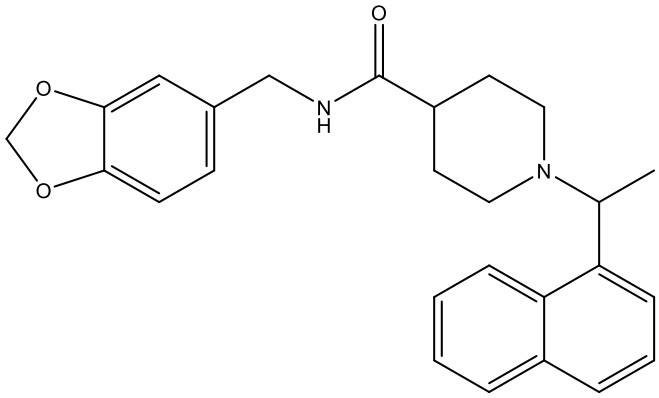

N-(benzo[*d*][1,3]dioxol-5-ylmethyl)-1-(1-(naphthalen-1-yl)ethyl)piperidine-4-carboxamide

Figure 3: 2-D structure of the first ligand (M3) with its IUPAC name used in the study

.

i. Gibb's Free Energy Calculations and Virtual Screening

A molecular interaction study was conducted to compute the scoring function and research protein-ligand interactions in predicting the binding affinity and biochemical activity of the ligand (Šinko, G. 2019; Naqvi *et al*., 2018). To estimate the binding affinity, Auto Dock Vina 4.2 of PyRx software was used, while visualization of protein-ligand interactions by non-bonding and hydrophobic interactions was explored using the 2016 version of Discovery Studio Visualizer software (Arthur *et al*., 2021). The protein (PDB ID: 5Y3Q) structure in pdb format was opened using the virtual screening instrument PyRx. The molecules were selected and automatically transformed into the pdb layout. The lattice box automatically appeared, and the center of the mark site was allocated along with the dimensions after both were chosen. The docking was achieved with the auto dock Vina to observe the precision of the docking situation.

ii. Retrieval of Receptor and Preparation Show

The receptor was prepared by downloading the 3D structure of the protein complex (PDB: 5Y3Q) from the Protein data Bank. The heteroatoms and water molecules of the receptors were manually removed from the downloaded 3D structure of the amino acid, and then saved in pdb file format as a refined/prepared receptor as shown in Figure.

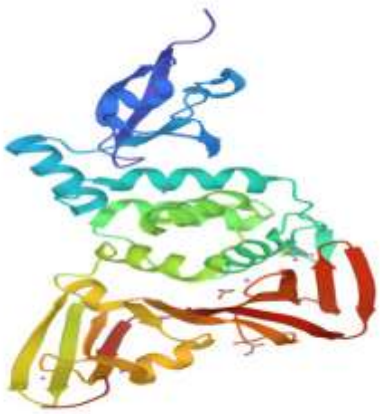

Figure 4**:** 3D structure of the receptor M1 (PDB ID: 5Y3Q) with a resolution of 1.65Å

Results and Discussions

Table 2: Quantitative description of the interaction of M1, M2 and their analogues on SARS-Cov2 receptor (PDB ID: 5Y3Q).

Nflex: - Number of rotatable torsions
Hbond: - hydrogen bond energy
Hphob: - hydrophobic energy in exposing a surface to water
Vwint: - The van der Waals interaction energy (sum of gc and gh van der Waals)
Eintl: - Internal conformational energy of the ligand

Dsolv: - The desolvation of exposed H-bond donors and acceptors
SolEl: - The solvation electrostatics energy change upon binding

The result shown in table 2, describes the result of all the ligands used in molecular docking study of 5Y3Q receptor. This study showed the least binding energy were M1c with – 20.418 kcal/mol, and M1b with -20.388 kcal/mol. These binding energies were found to be favorable for an efficient docking and resultant inhibition of the viral main protease. Rutwick and Surya in 2021 reported a molecular docking study result of Bioquercetin (Quercetin 3-O-robinobioside) with SARS COV2 receptor and the binding energy was found to be - 7.97 kcal/mol. The binding energies of M1c and M1b showed that M1c and M1b are better inhibitors of SARS COV2 than Bio-quercetin (Quercetin 3-O-robinobioside) reported by Rutwick and Surya, since their binding score is lower than that of bio-Quercetin reported in the literature.

However, the results of the binding energies show M3e and M3f with binding energy -8.22 and -10.289 kcal/mol respectively are the least unfavorable binding energies.

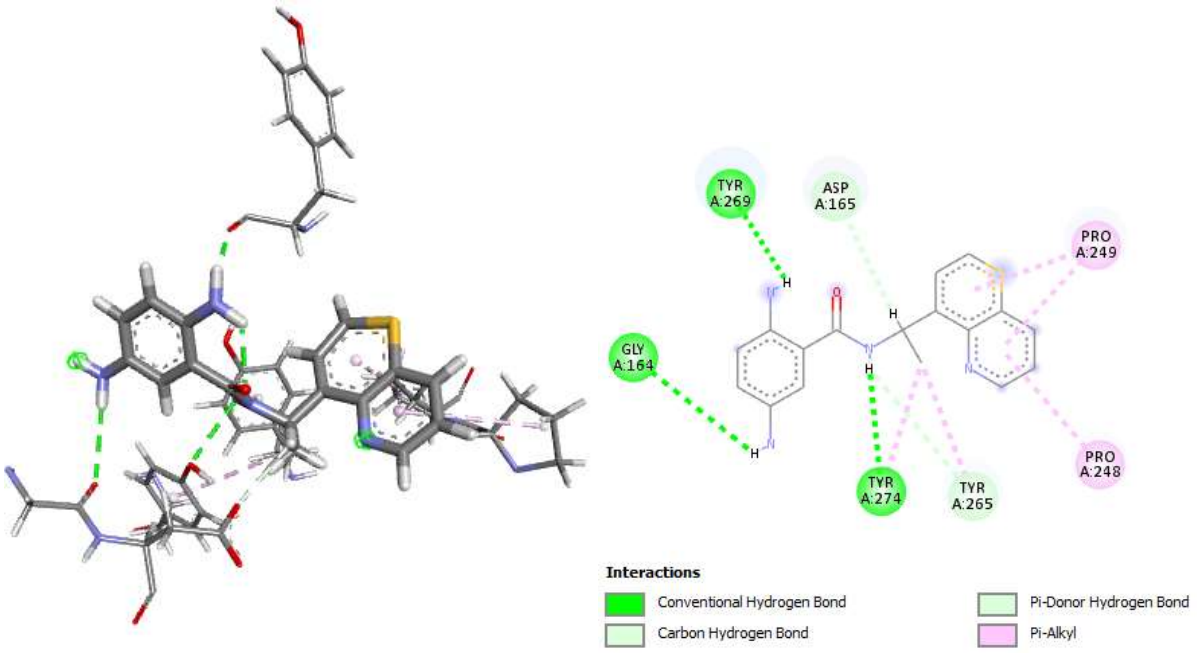

Figure 5**:** The 2D and 3D view of interaction type of M1 with surrounding amino acids of 5Y3Q.

The amino acids are shown in four different colors, the green color shows the conventional hydrogen bonds, pink shows the pi-alkyl, and the sky blue shows the carbon Hydrogen bond while the light blue shows the pi-donor hydrogen bonds.

Table 3: Interaction types and amino acids involved in the inhibition of SARS-Cov2 receptor (PDB ID: 5Y3Q) with M1 Inhibitor

Distance	Types	From	To
2.188	Conventional Hydrogen Bond	: M1:H20	A:GLU168:OE1
2.125	Conventional Hydrogen Bond	: M1:H5	A:ASP165:OD1
4.212	Pi-Anion	A:ASP165:OD1	: M1
2.606	Pi-Sigma	A:ASP165:HB1	: M1
3.255	Pi-Alkyl	A:TYR265	: M1:C3
5.145	Pi-Alkyl	A:TYR274	: M1:C3
4.567	Pi-Alkyl	: M1	A:PRO249
3.998	Pi-Alkyl	: M1	A:PRO249

Table 3 shows the result of the interaction type and the amino acids involved between the ligand (M1) and the SARS Cov2 receptor with the PDB ID of 5Y3Q. The conventional hydrogen bond formed between the ligand and some amino acids are shown on the table, which were found donated from : M1:H10, : M1:H15, : M1;H16 and : M1:H17. In chain A: TYR274: OH, A: GLY164: O, M1a 1:O1 and A: TYR269: O of the receptor. The type of bond formed at a distance of 2.61Å is carbon hydrogen bond, found donated from the amine group of M1:H6 in chain A: ASP165: ODI of the receptor to the H-acceptor of the M1. The type of bond formed at a distance of 3.18 Å is pi-donor hydrogen bond from: M1:H10 to the pi-orbital in M1a.

The presence of conventional hydrogen bonds between the ligands and the binding score of the receptor were primarily responsible for the addition of the interaction energy, and this interaction are shown in table2. Other stabilizing energy associated with the binding affinity of M1a was linked to Pi-alkyl, pi-donor hydrogen bond, Carbon hydrogen bond and conventional hydrogen bond interactions of the ligands with the hydrogen interactions within the complex.

Table 4: Interaction types and amino acids involved in the inhibition of SARS-CoV2 receptor (PDB ID: 5Y3Q) with M1a Inhibitor

Distance	Types	From	To
2.77	Conventional Hydrogen Bond	M1a:H10	A:TYR274:OH
2.77	Conventional Hydrogen Bond	M1a:H15	A: GLY164: O
2.04	Conventional Hydrogen Bond	M1aH16	M1a:O1
1.97	Conventional Hydrogen Bond	M1a:H17	A: TYR269: O
2.61	Carbon Hydrogen Bond	M1a:H6	A:ASP165:OD1
3.18	Pi-Donor Hydrogen Bond	M1a:H10	A:TYR265
3.51	Pi-Alkyl	A:TYR265	M1a:C10
5.09	Pi-Alkyl	A:TYR274	M1a:C10
4.07	Pi-Alkyl	M1a	A:PRO249
4.97	Pi-Alkyl	M1a	A:PRO248
4.95	Pi-Alkyl	M1a	A:PRO249

Table 4 shows the result of the interaction type and the amino acids involved between the ligand (M1a) and the Cov2 receptor with the PDB ID of 5Y3Q. The conventional hydrogen bond formed between the ligand and some amino acids are shown on the table, which were found donated from M1a: to the H-donor of A: TYR265: OH in chain A: GLY164:0 of the receptor. The type of bond formed at a distance of 3.18 is pi-donor hydrogen bond, found donated from the amino acid of M1a:H10 in chain A: TYR265 of the receptor to the pi-orbital of the M1a. The type of bond formed at a distance of 2.61Å C-H bond to the H-acceptor in M1a.

The binding score and the hydrogen bond of M1a are indicated in table 1 (-16.900kcal/mol and -3.356kcal/mol). The presence of conventional hydrogen bonds between the ligands and the binding score of the receptor were primarily responsible for the addition of the interaction energy, and this interaction are shown in table 4.

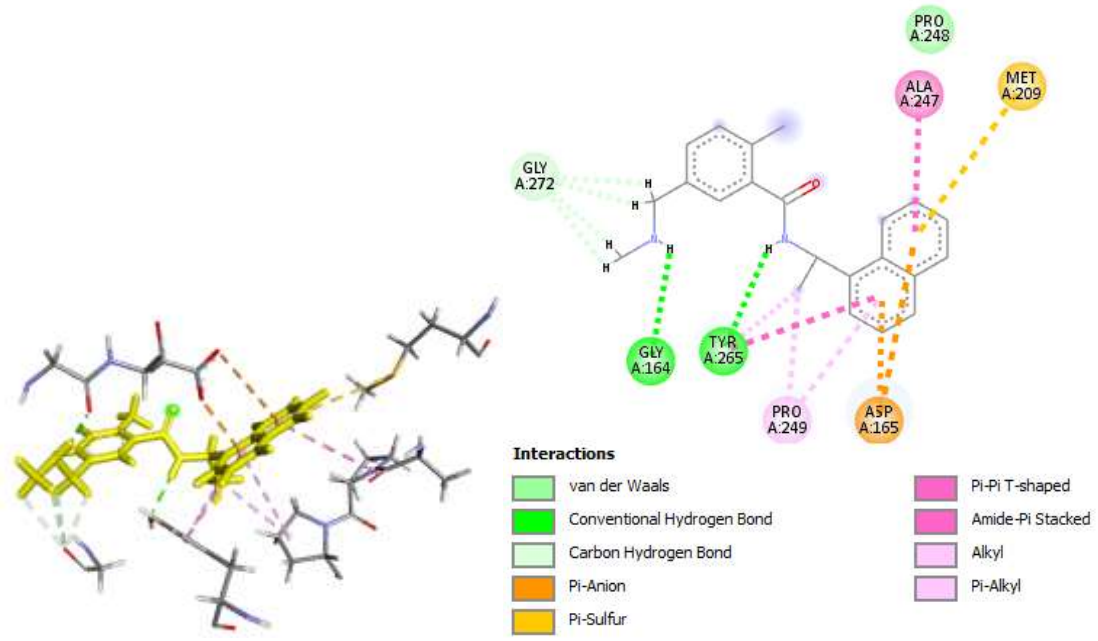

Figure 6**:** The 2D and 3D view of interaction type of M2 with surrounding amino acids of 5Y3Q.

The amino acids are shown in nine different colors the green color shows the conventional hydrogen bonds, yellow shows the pi-Sulfur, purple shows the pi-pi T-shaped, light green shows the Van der Waals, the orange color shows pi-Anion, the light blue shows the Carbon hydrogen bond, dark purple shows the Amide-Pi Stacked, light purple shows the Alkyl and the lighter purple shows the Pi-Alkyl.

Table 5: Interaction types and amino acids involved in the inhibition of SARS-CoV2 receptor (PDB ID: 5Y3Q) with M2 Inhibitor.

Distance	**Types**	**From**	**To**
2.11	Conventional Hydrogen Bond	M2:H2	A:TYR265:OH
2.06	Conventional Hydrogen Bond	M2:H21	A:GLY164:O
3.06	Carbon Hydrogen Bond	M2:H16	A:GLY272:O
2.65	Carbon Hydrogen Bond	M2:H17	A:GLY272:O
2.92	Carbon Hydrogen Bond	M2:H23	A: GLY272:O
2.97	Carbon Hydrogen Bond	M2:H24	A: GLY272:O
3.11	Pi-Anion	A:ASP165:OD1	M2
4.83	Pi-Anion	A:ASP165:OD2	M2
5.59	Pi-Sulfur	A:MET209:SD	M2

4.50	Pi-Pi T-shaped	A:TYR265	M2
5.03	Amide-Pi Stacked	A:ALA247:C,O;PRO248:N	M2
4.31	Alkyl	M2:C21	A:PRO249
4.49	Pi-Alkyl	A:TYR265	: M2:C21
5.06	Pi-Alkyl	M2	A:PRO249

Table 5 shows the result of the interaction type and the amino acids involved between the ligand (M2) and the Cov2 receptor with the PDB ID of 5Y3Q. The conventional hydrogen bond formed between the ligand and some amino acids are shown on the table. Four of these bonds can be seen between M2:H16 (3.06Å) and M2:H17 (2.65Å), M2:H23 (2.92Å), and M2:H24 (2.97 Å) formed an interaction with A: GLY272:0. The type of bond formed at a distance of 3.11 and 4.83 are pi-anion stacked bond found donated from negative (A: ASP165:OD1 and A: ASP165:0D2 to the: RES1.

The binding score and the hydrogen bond of M2 are indicated in table1 (-16.863kcal/mol and -2.941kcal/mol respectively). The presence of conventional hydrogen bonds between the ligands and the receptor were primarily responsible for the binding score of the complex, and this interaction are shown in table 5.

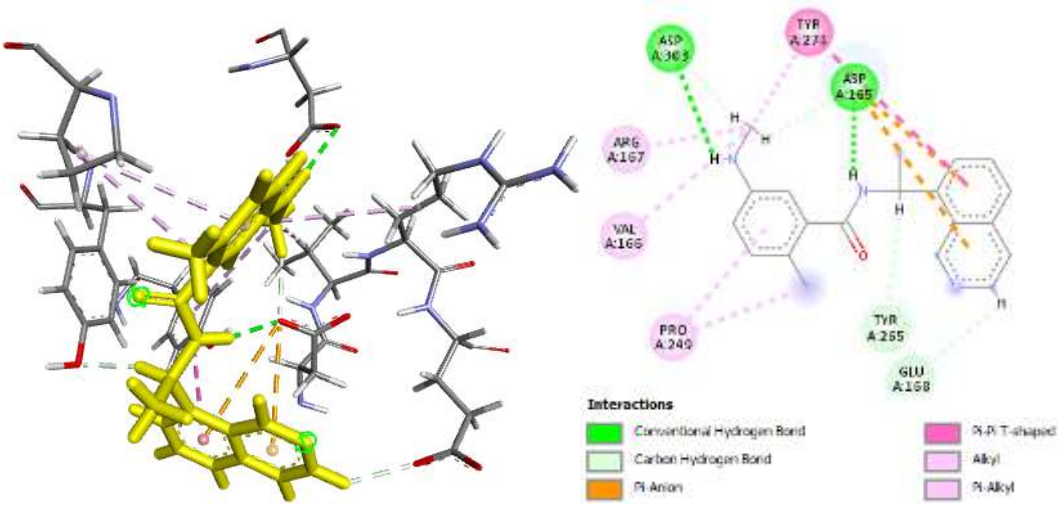

Figure 7**:** The 2D and 3D view of interaction type of M2a with surrounding amino acids of 5Y3Q.

The amino acids are shown in six different colors, the green color shows the conventional hydrogen bond, the pale green shows the carbon hydrogen bond and the orange shows pi-Anion, the purple shows the pi-pi T-shaped while the pale purple shows the Alkyl and Pi-Alkyl.

Table 6 shows the Interaction types and amino acids involved in the inhibition of SARS-Cov2 PLpro receptor (PDB ID: 5Y3Q) with M2a Inhibitor. The conventional hydrogen bond formed between the ligand and some amino acids are shown on the table. Four of these bonds can be seen between: M2a:H12 (2.15Å), M2a:H2O (2.47Å), M2a: HA (2.12Å) and M2a:H6 (2.34 Å). The type of bond formed at a distance2.15, 2.47, 2.12 and 2.34 are Carbon hydrogen bond found donated to the H-donor of the receptor M2a, the Pi-anion stacked interaction at a distance of 5.69 Å is found donated from negative to the pi-orbital of M2a, pi-alkyl bond is formed at a distance of 4.86, 4.63 and 4.65 Å were found donated from A: Val166 and A: ARG167 in chain of the receptor.

Table 6: Interaction types and amino acids involved in the inhibition of SARS-CoV2 receptor (PDB ID: 5Y3Q) with M2a Inhibitor.

Distance	Types	From	To
2.37	Conventional Hydrogen Bond	M2a:H11	A:ASP165:OD1
2.80	Conventional Hydrogen Bond	M2a:H7	A:ASP303:OD1
2.15	Carbon Hydrogen Bond	M2a:H12	A:TYR265:OH
2.47	Carbon Hydrogen Bond	M2a:H20	A:GLU168:OE1
2.12	Carbon Hydrogen Bond	M2a:H4	A:ASP303:OD2
2.34	Carbon Hydrogen Bond	M2a:H6	A:ASP165:OD1
4.54	Pi-Anion	A:ASP165:OD1	M2a
4.15	Pi-Anion	A:ASP165:OD1	M2a
5.69	Pi-Pi T-shaped	A:TYR274	M2a
4.86	Alkyl	M2a:C7	A:VAL166
4.63	Alkyl	M2a:C7	A:ARG167

4.65	Alkyl	M2a:C8	A:PRO249
5.38	Pi-Alkyl	A:TYR274	M1a:C7
4.89	Pi-Alkyl	M2a	A:PRO249

The binding score and the hydrogen bond of M2a are indicated in table1 (-17.723kcal/mol and -2.389kcal/mol). The presence of conventional hydrogen bonds were primarily responsible for the low free binding energy, and this interactions can be seen in table 4. Other stabilizing energy associated with the binding affinity of M2a was linked to, carbon hydrogen bond, pi-donor hydrogen bond, pi-pi stacked, amide-pi Alkyl and Pi-Alkyl interactions of M2a with the amino acids in the binding pockets of the receptor.

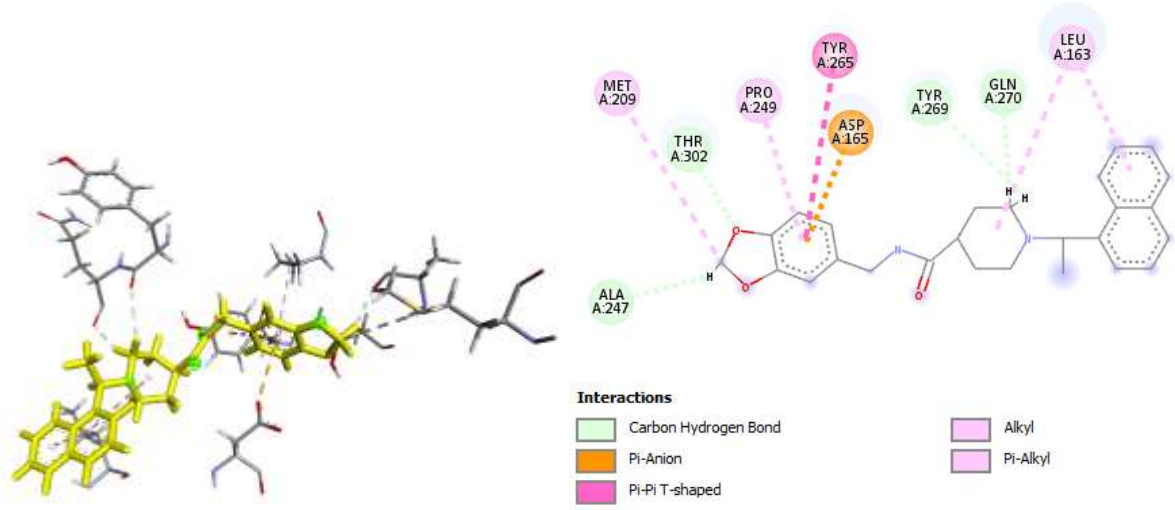

Figure 8: The 2D and 3D view of interaction type of M3 with surrounding amino acids of PDB ID: (5Y3Q). The amino acids are shown in five different colors, the light blue color shows the Carbon hydrogen bond, the orange shows the pi-Anion, purple shows the pi-pi T-shaped and the light purple shows the pi-alkyl and the alkyl.

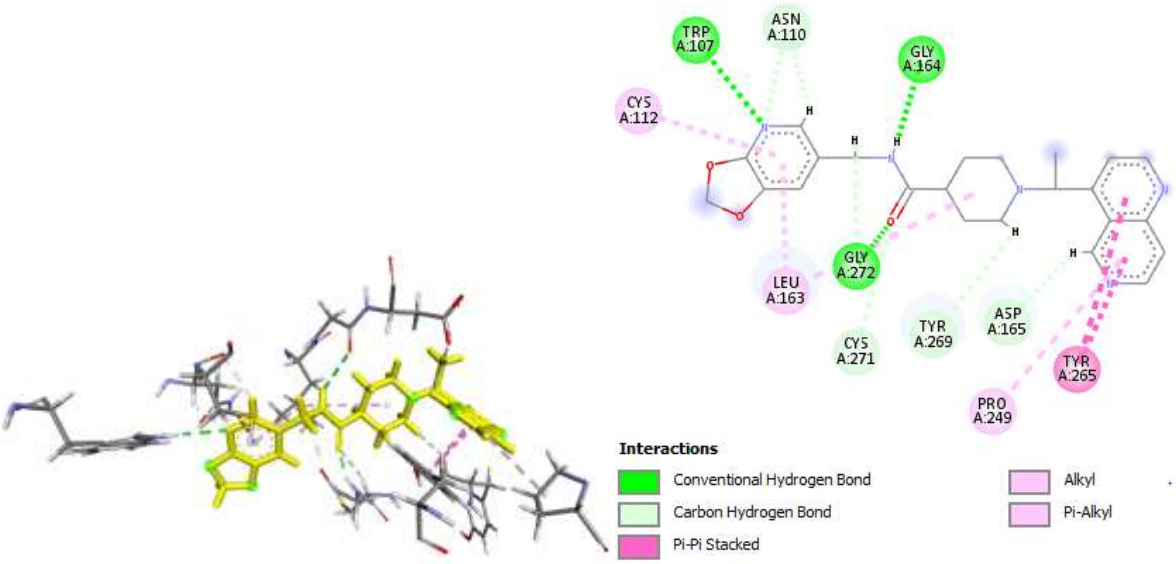

Figure 9: The 2D and 3D view of interaction type of M3a with surrounding amino acids of PDB ID 5Y3Q. The amino acids are shown in five different colors, the green color shows the conventional hydrogen bond, the light green shows the carbon hydrogen bond, purple shows the pi-pi shacked and the light purple shows the pi-alkyl and the alkyl.

Table 7: Interaction types and amino acids involved in the inhibition of SARS-CoV2 receptor (PDB ID: 5Y3Q) with M3a Inhibitor

Distance	Types	From	To
2.60	Conventional Hydrogen Bond	A:TRP107:HE1	M3:N1
1.63	Conventional Hydrogen Bond	A:GLY272:HN	M3:O3
2.94	Conventional Hydrogen Bond	:RES1:H7	A: GLY164: O
2.26	Carbon Hydrogen Bond	A:ASN110:HA	M3:N1
2.73	Carbon Hydrogen Bond	A:CYS271:HA	M3:O3
2.66	Carbon Hydrogen Bond	M3:H1	A: ASN110: O
2.80	Carbon Hydrogen Bond	M3:H11	A: TYR269: O
2.93	Carbon Hydrogen Bond	M3:H25	A:ASP165:OD1

Table 7 shows the Interaction types and amino acids involved in the inhibition of SARS-Cov2 receptor (PDB ID: 5Y3Q) with M3a Inhibitor. The conventional hydrogen bond formed between the ligand and some amino acids are shown on the table. Five of

these bonds can be seen between A: TYR274 (5.38Å), M3 (4.89Å), M3 (4.60Å), M3 (4.80Å), and M3 (5.23Å). A pi-pi T-shaped interaction formed at a distance of 5.69, and it was found donated from Alkyl to the pi-orbital.

The binding score and the hydrogen bond of M3a are specified in table1 (-12.125kcal/mol and -1.880kcal/mol). The existence of conventional hydrogen bonds between the ligands and the binding score of the receptor were principally accountable for the overall interaction energy, and this interaction are presented in table 7. Additional steadying energy linked with the binding affinity of M3a was associated with pi-pi shaped, Alkyl and Pi-Alkyl interactions of M3a within the complex.

Table 8: Chemical Structures of the Newly Designed compounds

M1	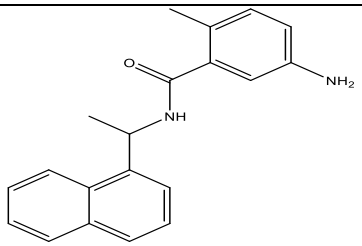	5-amino-2-methyl-*N*-(1-(naphthalen-1-yl)ethyl)benzamide
M1a	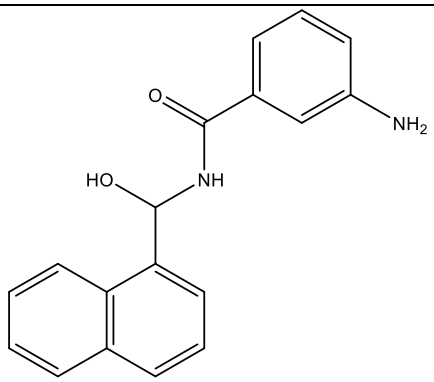	5-amino-2-hydroxy-N-(hydroxy(naphthalen-1-yl)methyl)benzamide
M1b	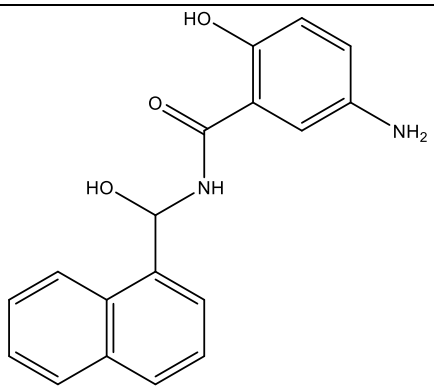	5-amino-2-hydroxy-N-(hydroxy(naphthalen-1-yl)methyl)benzamide

M1c	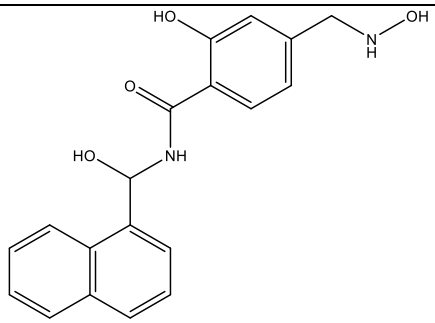	2-hydroxy-N-(hydroxy(naphthalen-1-yl)methyl)-4-((hydroxyamino)methyl)benzamide
M1d	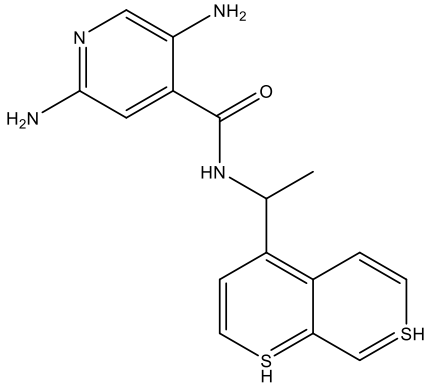	N-(1-(3l4,5l4-thiopyrano[3,2-d][1,3]thiazin-8-yl)ethyl)-2,5-diaminoisonicotinamide
M1e	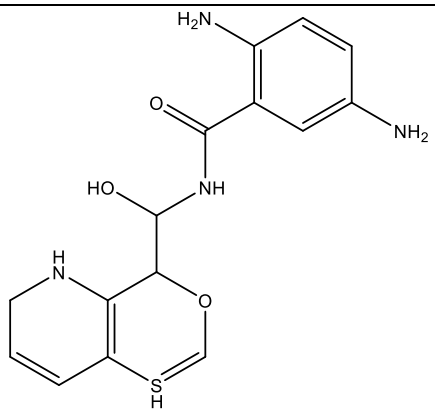	2,5-diamino-N-((5,6-dihydro-1l4-thiopyrano[3,2-b]pyridin-4-yl)(hydroxy)methyl)benzamide
M1f	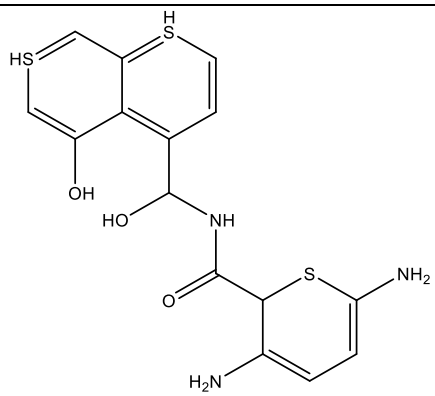	3,6-diamino-N-(hydroxy(5-hydroxyPC-1l4,7l4-thiopyrano[3,4-b]thiopyran-4-yl)methyl)-2H-thiopyran-2-carboxamide

M2	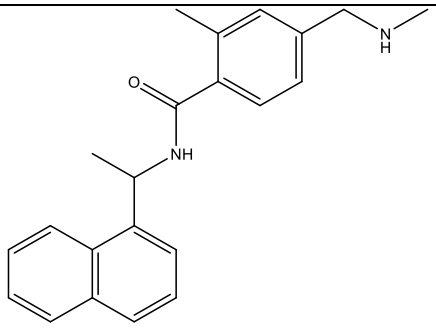	2-methyl-4-((methylamino)methyl)-N-(1-(naphthalen-1-yl)ethyl)benzamide
M2a	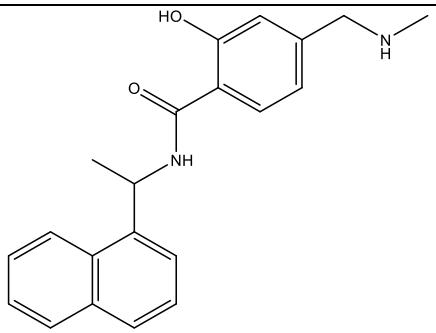	2-hydroxy-4-((methylamino)methyl)-N-(1-(naphthalen-1-yl)ethyl)benzamide
M2b	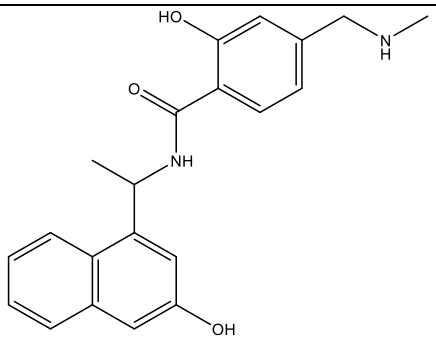	2-hydroxy-N-(1-(3-hydroxynaphthalen-1-yl)ethyl)-4-((methylamino)methyl)benzamide
M2c	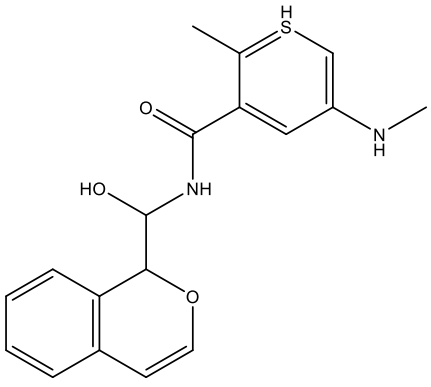	N-(hydroxy(1H-isochromen-1-yl)methyl)-2-methyl-5-(methylamino)-1l4-thiopyran-3-carboxamide

M1d	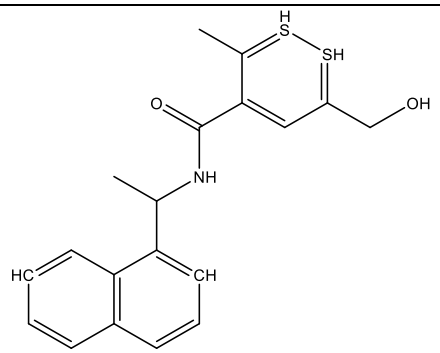	6-(hydroxymethyl)-3-methyl-N-(1-(naphthalen-1-yl)ethyl)-1l4,2l4-dithiine-4-carboxamide
M1e	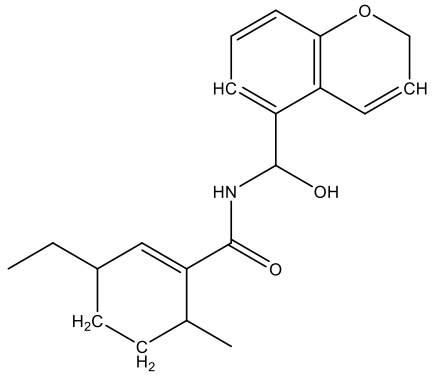	N-((2H-chromen-5-yl)(hydroxy)methyl)-3-ethyl-6-methylcyclohex-1-ene-1-carboxamide
M1f	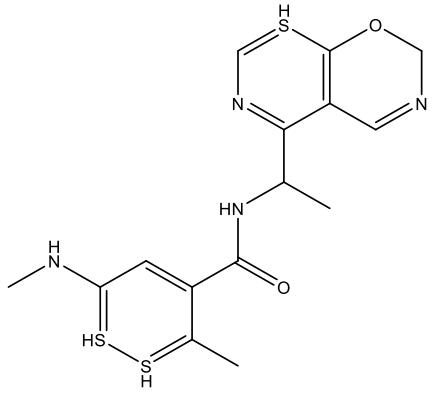	N-(1-(2H-8l4-[1,3]thiazino[5,6-e][1,3]oxazin-5-yl)ethyl)-3-methyl-6-(methylamino)-1l4,2l4-dithiine-4-carboxamide
M3	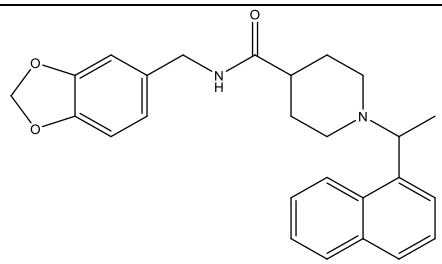	N-(benzo[d][1,3]dioxol-5-ylmethyl)-1-(1-(naphthalen-1-yl)ethyl)piperidine-4-carboxamide
M3a	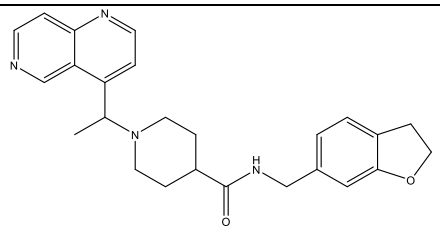	1-(1-(1,6-naphthyridin-4-yl)ethyl)-N-((2,3-dihydrobenzofuran-6-yl)methyl)piperidine-4-carboxamide

M3b	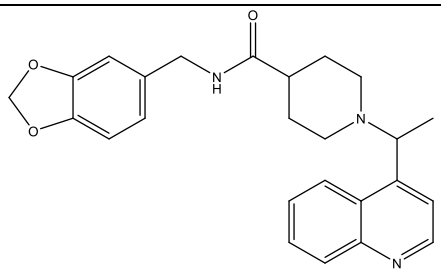	N-(benzo[d][1,3]dioxol-5-ylmethyl)-1-(1-(quinolin-4-yl)ethyl)piperidine-4-carboxamide
M3c	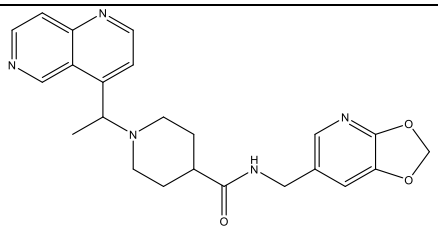	1-(1-(1,6-naphthyridin-4-yl)ethyl)-N-([1,3]dioxolo[4,5-b]pyridin-6-ylmethyl)piperidine-4-carboxamide
M3d	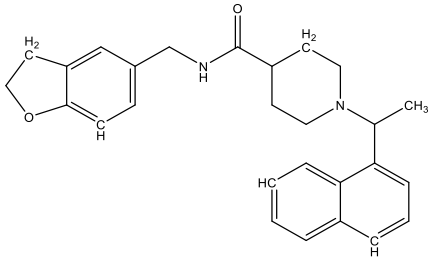	N-((2,3-dihydrobenzofuran-5-yl)methyl)-1-(1-(naphthalen-1-yl)ethyl)piperidine-4-carboxamide
M1e	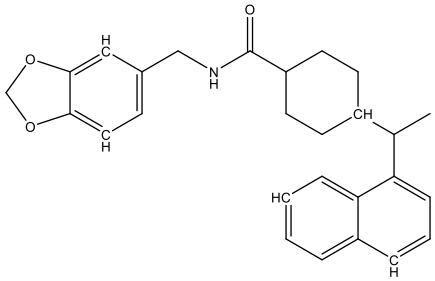	N-(benzo[d][1,3]dioxol-5-ylmethyl)-4-(1-(naphthalen-1-yl)ethyl)cyclohexane-1-carboxamide
M1f	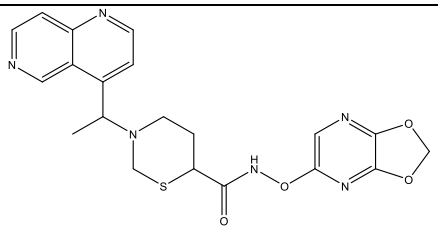	3-(1-(1,6-naphthyridin-4-yl)ethyl)-N-([1,3]dioxolo[4,5-b]pyrazin-5-yloxy)-1,3-thiazinane-6-carboxamide

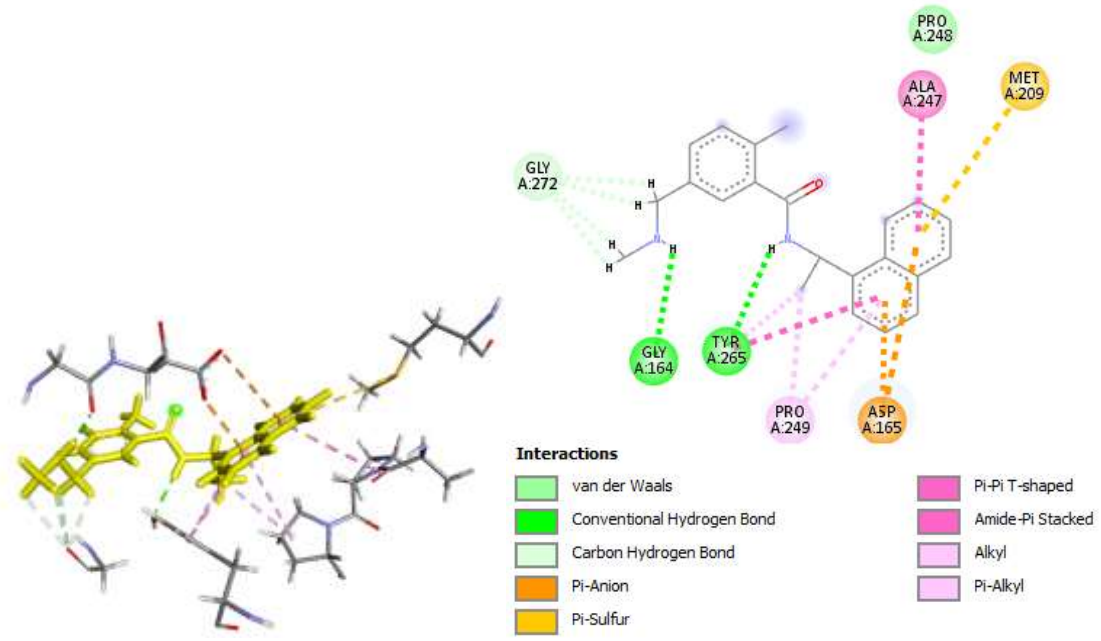

Figure 10: The 2D and 3D view of interaction type of M2 with surrounding amino acids of 5Y3Q

The amino acids are shown in nine different colors the green color shows the conventional hydrogen bonds, yellow shows the pi-Sulfur, purple shows the pi-pi T-shaped, light green shows the Van der Waals, the orange color shows pi-Anion, the light blue shows the Carbon hydrogen bond, dark purple shows the Amide-Pi Stacked, light purple shows the Alkyl and the lighter purple shows the Pi-Alkyl.

Table 8: Interaction types and amino acids involved in the inhibition of SARS-COv2 receptor (PDB ID: 5Y3Q) with M2 Inhibitor

Distance	Types	From	To
2.11	Conventional Hydrogen Bond	M2:H2	A:TYR265:OH
2.06	Conventional Hydrogen Bond	M2:H21	A:GLY164:O
3.06	Carbon Hydrogen Bond	M2:H16	A:GLY272:O
2.65	Carbon Hydrogen Bond	M2:H17	A:GLY272:O
2.92	Carbon Hydrogen Bond	M2:H23	A:GLY272:O
2.97	Carbon Hydrogen Bond	M2:H24	A:GLY272:O
3.11	Pi-Anion	M2:OD1	M2
4.83	Pi-Anion	M2:OD2	M2
5.59	Pi-Sulfur	M2:SD	M2
4.50	Pi-Pi T-shaped	A:TYR265	M2
5.03	Amide-Pi Stacked	A:ALA247:C,O;PRO248:N	M2
4.31	Alkyl	M2:C21	A:PRO249
4.49	Pi-Alkyl	A:TYR265	M2:C21
5.06	Pi-Alkyl	M2	A:PRO249

Table 8 shows the result of the interaction type and the amino acids involved between the ligand (M2) and the SARS-Cov2 receptor with the PDB ID of 5Y3Q. The conventional hydrogen bond formed between the ligand and some amino acids are shown on the table. Four of these bonds can be seen between M2:H16 (3.06Å) and M2:H17 (2.65Å), M2:H23 (2.92Å) AND M2:H24 (2.97 Å) formed an interaction with A: GLY272:0. The type of bond formed at a distance of 3.11 and 4.83 are pi-anion stacked bond found donated from negative (A: ASP165:OD1 and A: ASP165:0D2 to the: M2.

The binding score and the hydrogen bond of M2 are indicated in table1 (-16.863kcal/mol and -2.941kcal/mol respectively). The presence of conventional hydrogen bonds between the ligands and the receptor were primarily responsible for the binding score of the complex, and this interaction are shown in table 1 other stabilizing energy associated with the binding affinity of M2 was linked to Carbon hydrogen bond, pi-alkyl and Alkyl interactions of the ligands with the hydrogen bond interaction within the complex.

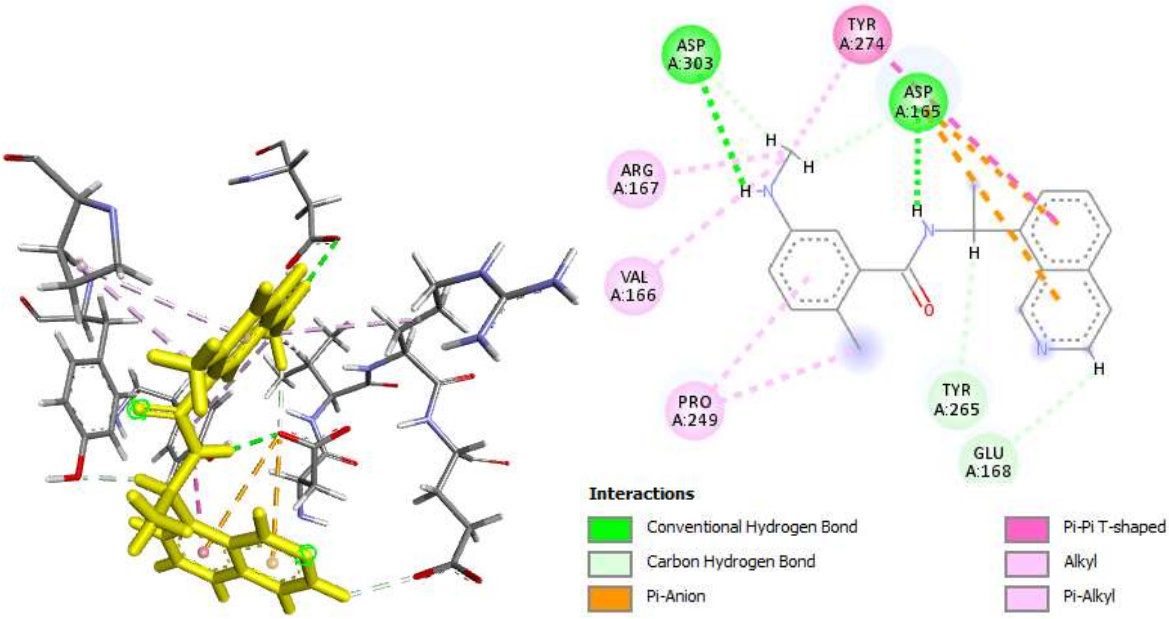

Figure 11: The 2D and 3D view of interaction type of M2a with surrounding amino acids of 5Y3Q.The amino acids are shown in six different colors, the green color shows the conventional hydrogen bond, the pale green shows the carbon hydrogen bond and the orange shows pi-Anion, the purple shows the pi-pi T-shaped while the pale purple shows the Alkyl and Pi-Alkyl.

Table 9: Interaction types and amino acids involved in the inhibition of SARS-CoV2 PLpro receptor (PDB ID: 5Y3Q) with M2a Inhibitor

Distance	Types	From	To
2.37	Conventional Hydrogen Bond	M2a:H11	A:ASP165:OD1
2.80	Conventional Hydrogen Bond	M2a:H7	A:ASP303:OD1
2.15	Carbon Hydrogen Bond	M2a:H12	A:TYR265:OH
2.47	Carbon Hydrogen Bond	M2a:H20	A:GLU168:OE1
2.12	Carbon Hydrogen Bond	M2a:H4	A:ASP303:OD2
2.34	Carbon Hydrogen Bond	M2a:H6	A:ASP165:OD1
4.54	Pi-Anion	A:ASP165:OD1	M2a
4.15	Pi-Anion	A:ASP165:OD1	M2a
5.69	Pi-Pi T-shaped	A:TYR274	M2a
4.86	Alkyl	M2a	A:VAL166
4.63	Alkyl	M2a	A:ARG167
4.65	Alkyl	M2a:C8	A:PRO249
5.38	Pi-Alkyl	A:TYR274	M2a:C7
4.89	Pi-Alkyl	M2a	A:PRO249

Table 9 shows the Interaction types and amino acids involved in the inhibition of SARS-Cov2 PLpo receptor (PDB ID: 5Y3Q) with M2a Inhibitor. The conventional hydrogen bond formed between the ligand and some amino acids are shown on the table. Four of these bonds can be seen between: M2a:H12 (2.15Å), M2a:H2O (2.47Å), M2a: HA (2.12Å) and M2a:H6 (2.34 Å). The type of bond formed at a distance2.15, 2.47, 2.12 and 2.34 are Carbon hydrogen bond found donated to the H-donor of the receptor M2a, the Pi-anion stacked interaction at a distance of 5.69 Å is found donated from negative to the pi-orbital of M2a, pi-alkyl bond is formed at a distance of 4.86, 4.63 and 4.65 Å were found donated from A: Val166 and A: ARG167 in chain of the receptor.

The binding score and the hydrogen bond of M2a are indicated in table1 (-17.723kcal/mol and -2.389kcal/mol). The presence of conventional hydrogen bonds were primarily responsible for the low free binding energy, and this interactions can be seen in table 4. Other stabilizing energy associated with the binding affinity of LIG2C was linked to, carbon hydrogen bond, pi-donor hydrogen bond, pi-pi stacked, amide-pi Alkyl and Pi-Alkyl interactions of M2a with the amino acids in the binding pockets of the receptor.

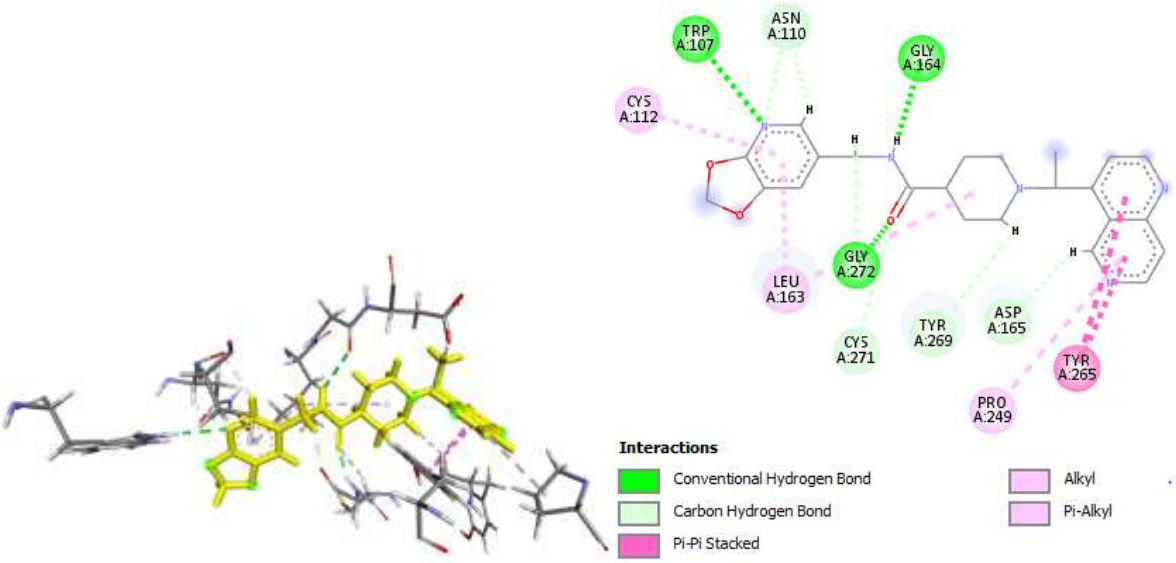

Figure 12: The 2D and 3D view of interaction type of M3a with surrounding amino acids of PDB ID 5Y3Q.

The amino acids are shown in five different colors, the green color shows the conventional hydrogen bond, the light green shows the carbon hydrogen bond, purple shows the pi-pi shacked and the light purple shows the pi-alkyl and the alkyl.

Table 10**:** Interaction types and amino acids involved in the inhibition of SARS-Cov2 receptor (PDB ID: 5Y3Q) with M3 Inhibitor

Distance	**Types**	**From**	**To**
2.60	Conventional Hydrogen Bond	A:TRP107:HE1	M3a:N1
1.63	Conventional Hydrogen Bond	A:GLY272:HN	M3a::O3
2.94	Conventional Hydrogen Bond	: M3a:H7	A: GLY164: O
2.26	Carbon Hydrogen Bond	A:ASN110:HA	: M3a:N1
			M3a::O3
2.73	Carbon Hydrogen Bond	A:CYS271:HA	
2.66	Carbon Hydrogen Bond	M3a:H1	A: ASN110: O
2.80	Carbon Hydrogen Bond	M3a::H11	A: TYR269: O
2.93	Carbon Hydrogen Bond	M3a::H25	A:ASP165:OD1
1.98	Carbon Hydrogen Bond	M3a::H6	A: GLY272: O
5.97	Pi-Pi Stacked	A:TYR265	M3a:
4.05	Pi-Pi Stacked	A:TYR265	M3a
5.35	Alkyl	A:LEU163	M3a:
4.60	Pi-Alkyl	M3a:	A:CYS112
4.80	Pi-Alkyl	M3a:	A:LEU163
5.23	Pi-Alkyl	M3a:	A:PRO249

Table10 shows the Interaction types and amino acids involved in the inhibition of Cov2 receptor (PDB ID: 5Y3Q) with M3a Inhibitor. The conventional hydrogen bond formed between the ligand and some amino acids are shown on the table. five of these bonds can be seen between A:TYR274 (5.38Å), : M3a: (4.89Å),M3a: (4.60Å), M3a: (4.80Å), and M3a: (5.23Å). A pi-pi T-shaped interaction formed at a distance of 5.69, and it was found donated from Alkyl to the pi-orbital.

The binding score and the hydrogen bond of M3a are specified in table1 (-12.125kcal/mol and -1.880kcal/mol). The existence of conventional hydrogen bonds between the ligands and the binding score of the receptor were principally accountable for the overall interaction energy, and this interaction are presented in table 7. Additional steadying energy linked with the binding affinity of M3a was associated with pi-pi shaped, Alkyl and Pi-Alkyl interactions of M3a within the complex.

The docking results presented in Table 2 provide an extensive quantitative description of the interactions between M1, M2, their analogues, and the SARS-CoV-2 receptor (PDB ID: 5Y3Q). These interactions are assessed based on multiple parameters such as docking scores, hydrogen bond energies, hydrophobic interactions, van der Waals forces, internal conformational energies, and solvation-related effects. The findings reveal significant differences in the binding efficiencies and interaction profiles of the inhibitors tested. Among the tested inhibitors, M1b (-20.388) and M1c (-20.419) exhibit the lowest docking scores, suggesting the highest binding affinity to the receptor. M1f also exhibits a strong binding score (-20.361), further supporting the potential of M1 analogues as effective inhibitors. In contrast, M3e (-8.220) shows the least favorable docking score, indicating a weaker interaction with the target receptor.

The hydrogen bond energies (Hbond) vary significantly among the compounds, with M1f (-5.789) demonstrating the strongest hydrogen bonding potential, while others such as M3 and M3e have relatively weak hydrogen bonding contributions. Strong hydrogen bonding interactions often contribute to ligand stability and specificity in binding. Hydrophobic interactions (Hphob) and van der Waals interactions (Vwint) are crucial in stabilizing the inhibitor-receptor complex. The compounds with high van der Waals interaction values, such as M3a (-31.663) and M3d (-30.411), suggest extensive surface complementarity with the receptor, potentially enhancing binding affinity.

Desolvation energy (Dsolv) and solvation electrostatics energy (SolEI) further illustrate the influence of solvation effects on binding. Notably, M1f (17.909) and M3c (18.897) exhibit the highest desolvation energy, indicating a significant energy cost in desolvation upon binding, while M3a (24.502) shows the highest solvation electrostatics energy, which might influence the stability of the complex.

Tables 3-10 detail the interaction types and amino acids involved in inhibitor binding. Hydrogen bonding is consistently observed with residues such as GLY164, TYR265, ASP165, and GLU168. Pi-alkyl interactions are notably present with residues such as PRO249, TYR265, and TYR274, contributing to the ligand stability within the receptor binding site. Pi-anion and pi-pi

stacking interactions further stabilize the inhibitor-receptor complex, particularly in M1a, M2, and M3 analogues.

Overall, the results indicate that M1 and its analogues demonstrate significant potential as SARS-CoV-2 inhibitors due to their strong docking scores, extensive hydrogen bonding, and favorable van der Waals and hydrophobic interactions. M2 and its analogues also exhibit promising interactions but with slightly lower binding scores compared to M1 analogues. M3 and its derivatives show moderate binding interactions, with variations in their hydrogen bonding and hydrophobic interactions.

The computational docking analysis highlights M1 and its analogues as the most promising inhibitors against the SARS-CoV-2 receptor (PDB ID: 5Y3Q). The high binding affinity, strong hydrogen bonding, and stable hydrophobic interactions observed for M1b, M1c, and M1f suggest that these compounds could serve as lead candidates for further in vitro and in vivo evaluations.

The study also underscores the importance of hydrogen bonding and van der Waals interactions in stabilizing ligand-receptor complexes. Pi-anion and pi-alkyl interactions with critical residues such as ASP165, TYR265, and PRO249 play a vital role in binding efficacy. The solvation and desolvation energies further influence the stability and binding efficiency of these inhibitors. While M2 and its analogues show favourable docking scores and interactions, they demonstrate slightly lower binding affinity compared to M1 derivatives. M3 analogues exhibit moderate interaction potential, with some derivatives displaying weaker docking scores and fewer hydrogen bonding interactions.

Future studies should focus on molecular dynamics simulations and experimental validation to confirm these computational findings. Structural modifications based on the interaction profiles observed in this study could further enhance binding efficiency and optimize these inhibitors for therapeutic application against SARS-CoV-2.

References

Agarwal S, Jangir DK, Mehrotra R, Lohani N, Rajeswari M (2014) A Structural Insight into Major Groove Directed Binding of Nitrosourea Derivatives Nimustine with DNA: A Spectroscopic Study. *Plos ONE*, 9: 104-115

Arthur, D. E., Akoji, J. N., Sahnoun, R., Okafor, G. C., Abdullahi, K. L., Abdullahi, S. A., and Mgbemena, C. (2021). A Theoretical Insight in Interactions of Some Chemical Compounds as Mtor Inhibitors. *Bulletin of the National Research Centre*, *45*(1), 1-12.

Arthur, D. E., Ejeh, S., and Uzairu, A. (2020). Quantitative Structure-Activity Relationship (Qsar) and Design of Novel Ligands That Demonstrate High Potency and Target Selectivity as Protein Tyrosine Phosphatase 1b (Ptp 1b) Inhibitors as an Effective Strategy Used to Model Anti-Diabetic Agents. *Journal of Receptors and Signal Transduction, 40*(6), 501-520.

Cho, J.K., Curtis-Long, M.J., Lee, K.H., Kim, D.W., Ryu, H.W., Yuk, H.J., Park, K.H.(2013) Geranylated flavonoids displaying SARS-CoV papain-like protease inhibition from the fruits of Paulownia tomentosa. Bioorg. *Medicinal Chemistry*. 21, 3051–3057.

Clemente, V., D'Arcy, P., and Bazzaro, M. (2020). Deubiquitinating enzymes in coronaviruses and possible therapeutic opportunities for COVID-19. *International Journal of Molecular Sciences*. 21:3492. doi: 10.3390/ijms21103492

Hsih, W.H., Cheng, M.-Y., Ho, M.W., Chou, C.H., Lin, P.-C., Chi, C.-Y.. (2020). Featuring COVID-19 cases via screening symptomatic patients with epidemiologic link during flu season in a medical center of central Taiwan. *Journal of Microbiology Immunology and Infection*. 53, 459–466. doi: 10.1016/j.jmii.2020.03.008

protease against phytochemicals of Boerhavia diffusa

Linn. For novel COVID-19 drug discovery. Indian virological society. 32(1):46–54

Salmaso, V and Moro, s. (2018). Molecular docking to molecular dynamics in exploring ligand protein recognition process: An overview. *Frontiers in pharmacology*. 9,1-3

Ibrahim, M. T., Ismail, M. I., Bauer, M. R,. Bekhit, A.A ., Boeckler, F. M.2 (2020). Supporting SARS-CoV-2 Papain-Like Protease Drug Discovery: In silico Methods and Benchmarking. *Frontier in Chemistry*, 8:2-8

Li, X., Geng, M., Peng, Y., Meng, L., and Lu, S. (2020a). Molecular immune pathogenesis and diagnosis of COVID-19. *Journal Pharmaceutical Analysis*. 10: 102–108. doi: 10.1016/j.jpha.2020.03.001

Li, X., Wang, W., Zhao, X., Zai, J., Zhao, Q., Li, Y., *et al*. (2020b). Transmission dynamics and evolutionary history of 2019-nCoV. *Journal Medical Virology*. 92, 501–511. doi: 10.1002/jmv.25701

Rutwick , S. U , and Praveen, U. (2021). A molecular docking study of SARS-CoV-2 main